CrossMark

An Implicit Finite Difference Model for Electrokinetic Remediation of Cd-Spiked Kaolinite Under Acid-Enhanced and Unenhanced Conditions

Milad Rezaee [1] · Gholamreza Asadollahfardi [1]

Abstract

A numerical model based on an implicit finite difference method is presented to describe multi-species transport in cadmium-contaminated kaolin under electrokinetic remediation process. A set of algebra and partial differential equations were used to mathematically describe the reactive transport of the target species. We considered different coupled transport phenomena such as diffusion, electroosmotic flow, and ionic migration. Geochemical and electrochemical reactions including precipitation/dissolution, adsorption/desorption, water auto ionization, and electrolysis in anode and cathode cells were included in the model. Simulation results were compared with the available experimental data for electrokinetic remediation of cadmium-contaminated kaolinite. The coefficient of determination (R^2) and index of agreement (IA) were calculated to indicate the model accuracy and to compare the present model with the existing explicit finite difference model in the literature. The R^2 and IA calculation described that the present model had a good capability of simulating the experimental measurement. In addition, it illustrated that the presented implicit finite difference model had a better simulation result than the explicit model. The sensitivity analysis was conducted to understand the impact of tortuosity and retardation factors on the model output. Sensitivity analysis indicated that instead of the acid-enhanced test, the retardation factor had more impact on the unenhanced test. In addition, the sensitivity analysis of tortuosity factor revealed that this parameter had more significant effect on the cadmium concentration rather than pH profile.

Keywords Numerical model · Finite difference · Electrokinetic remediation · Geochemical reactions · Cadmium · Sensitivity analysis

1 Introduction

Soil pollution is a common and serious problem for the environment in all over the world. One of the most common pollutions is heavy metal, and evidence of soil pollution by heavy metal was found in Europe, the USA, and Asia [1]. Several different technologies have been developed to remediate soils, sediments, and groundwater based on physicochemical, thermal, and biological principles [2]. However, they are often found to be costly, energy-intensive, ineffective, and could themselves create other adverse environmental impacts when dealing with difficult subsurface and contaminant conditions

[3]. Electrokinetic remediation (EKR) consists of the application of an electric field into the soil, producing the migration of the organic and inorganic contamination through the porous medium. During the EKR treatment, the applied current causes oxidation at the anode and reduction at the cathode then leads to a series of coupled transport phenomena (ionic migration, electroosmotic flow, and electrophoresis); consequently, the pollutants are enriched near the electrodes and removed from the soil [4]. Ionic contaminants will move towards the electrode with opposite charge (anions towards the anode and cations towards the cathode) by ionic migration, while organic matters will mainly move due to electroosmotic flow [5]. Electrophoresis becomes significant in the EKR when surfactants are used to enhance the EKR process, or when the technique is employed in the remediation of slurries [6].

Several fundamental studies on EKR processes have been carried out to better understand the basis of the technique. Jacobs et al. introduced a model for EKR of zinc-

---

✉ Gholamreza Asadollahfardi
  fardi@khu.ac.ir

[1] Department of Civil Engineering, Kharazmi University, Tehran, Iran

contaminated soil. Their model was based on the convection-diffusion equation, and they stated a good agreement between their model and the experiment [7]. Alshawabkeh and Acar developed a numerical model for electrokinetic decontamination of lead-contaminated kaolinite, and they asserted that lead concentration and pH profiles predicted by their model had a fairly well agreement with the experimental data [8]. Haran et al. focused on modeling EKR of hexavalent chromium-contaminated sandy soil. They ignored the electroosmotic flow because of the low surface charge of the sand and reached a reasonable agreement between the prediction and the experimental measurement [9]. Kim et al. [10] represented a model for predicting cadmium concentration across the kaolinite, and Kim et al. [11] presented another model for simulation of EKR of lead-contaminated kaolinite soil. The predicted pollution concentration and pH profile were in a sensible agreement with their experimental data. Park et al. proposed a numerical model for remediation of phenol-contaminated kaolinite under electrokinetic process, and they reported a good agreement between the model and the experimental results [12]. Al-Hamdan and Reddy developed a one-dimensional transport model to simulate the transport and speciation of heavy metals (chromium, nickel, and cadmium) in the soil during the unenhanced EKR. Their model was incorporated with geochemical reactions, and they stated that their predictions had a reasonable agreement with the bench-scale tests [13]. Paz-García et al. introduced a model based on the Nernst–Planck–Poisson system of equations. They indicated that their model could predict the EKR process in both constant electric current density or in the constant difference of voltage [14]. Through using EKR method, Yeung et al. modeled remediation of lead-contaminated Georgia and Milwhite kaolinites and claimed that their model was capable of modeling the remediation process [15]. Paz-Garcia et al. modeled the transport of chemical species in porous material of soil, and they predicted lead and copper concentration profiles. Their results showed an overestimation in pH prediction, and they mentioned this phenomenon could have been due to the miscalculation of electric field strength, effective ionic mobility, and/or improper handling of soil pore fluid chemistry [16]. Asadollahfardi et al. proposed a numerical model for unenhanced EKR of lead-contaminated soil, and they reported good agreement between their predictions and experiments [17].

Various mathematical models have been proposed for unenhanced EKR [8, 9, 13, 14, 17] and acid-enhanced EKR [10–12, 16]. For the purpose of numerical modeling, finite element methods (FEM) [8, 14, 16] and finite difference methods (FDM) [10–13, 17] have been used by researchers. Most of the finite difference models were based on explicit schemes. Al-Hamdan and Reddy used implicit

FDM to simulate the unenhanced EKR and implemented simplified boundary conditions in their model and ignored the flux at the boundaries [13].

This paper presents an implicit finite difference model for modeling EKR of cadmium-contaminated kaolinite under acid-enhanced and unenhanced conditions. Chemical reactions such as precipitation/dissolution, adsorption/desorption, and water autoionization reaction were considered in the present model. The realistic boundary conditions with consideration of the effects of electrolysis reaction and flux at boundaries were utilized. Moreover, sensitivity analysis on retardation and tortuosity factors were carried out.

2 Materials and Methods

2.1 The Experimental Data

3To validate our numerical model, we compared our model results with Kim et al.'s [10] experimental data. The kaolinite soil was artificially contaminated by $Cd(NO_3)_2$ solution. For the acid-enhanced treatment, the electrolytes in the electrode compartments were 0.001 M HNO_3 solution for the anode and 0.1 M HNO_3 solution for the cathode. Figure 1 illustrates the schematic of the experimental apparatus. The experimental pilot consisted of four main parts: soil cell, electrode reservoir, electrolyte solution reservoirs, and power supply [10]. The soil cell dimension is $10 \times 10 \times 15$ cm with a volume of 1500 cm^3. On both sides of the soil cell, two sheets of porous polyethylene-terephthalate (PET) filter were inserted to prevent soil particles entering into the electrode reservoir. Platinum plate (10×10 cm) was used as the anode to prevent the introduction of extraneous products due to electrolytic reaction of the electrode surface, whereas a titanium plate (10×10 cm) was used as the cathode. The electrode reservoir contained 500 ml of electrolyte solution, ensuring that sufficient volume was present to avoid sudden variations of electrolyte solution [10]. Table 1 indicates the experimental data.

2.2 Transport Phenomena

As indicated in Fig. 1, the pilot contains two electrode cells on the sides of the contaminated soil sample The transportation of chemical species is mainly towards the anode and the cathode due to different transport phenomena. Electrode arrangement is the main factor that determines how the model should be considered. In this form of electrode arrangement (Fig. 1), chemical species transportation is mainly towards the anode (X = 0) and the cathode (X = L) cells (as a line), and it is possible to take into account the model one dimensional. Moreover, the experimental data for the cadmium concentration and pH are available as a line (one

Fig. 1 Schematic of the experimental apparatus
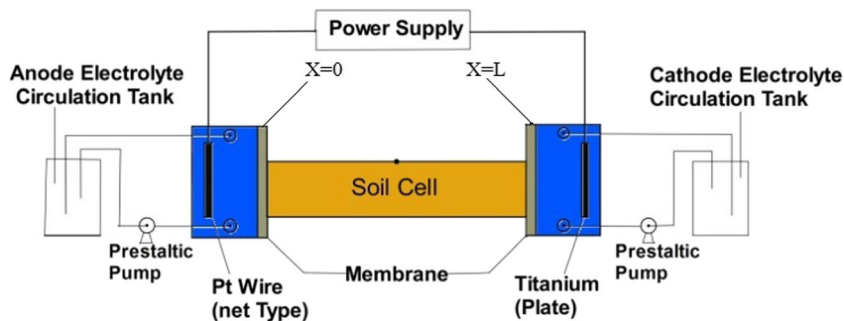
dimensional) between the anode and the cathode cells. Therefore, similar to previous works [10–13, 15], the present model is considered one dimensional.

A set of partial differential equations (PDEs) and algebraic equations are used to mathematically describe the reactive transport of the target species, which are H^+, OH^-, Cd^{2+}, and NO_3^-.

The flux of chemical species through a soil under the effect of chemical and electric potential gradient can be defined as a combination of diffusion, electroosmotic flow, and ionic migration [18–20], as

$$J_i = -D_i^{\text{eff}} \nabla c_i - c_i \left(u_i^{\text{eff}} + k_{eo} \right) \nabla \varnothing, \tag{1}$$

$$D_i^{\text{eff}} = n\tau D_i \tag{2}$$

where D_i^{eff} ($m^2\ s^{-1}$) is the effective diffusion coefficient, n ($-$) is the porosity of the soil, τ ($-$) is the tortuosity, u_i^{eff} ($m^2\ V^{-1}\ s^{-1}$) is the effective ionic mobility, k_{eo} ($m^2\ V^{-1}\ s^{-1}$) is the electroosmotic permeability, $\varnothing = \varnothing(x, t)$ (V) is the electric potential, and $c_i = c_i(x, t)$ (mol m^{-3}) is the concentration. For estimating effective ionic mobility, we used the Nernst-Einstein relation [18, 20, 21]:

$$u_i^{\text{eff}} = \frac{z_i F}{RT} D_i^{\text{eff}} \tag{3}$$

Table 1 Experimental parameter used in the present study [10]

	Unenhanced	Enhanced
Soil specimen	Kaolinite	
Contamination	Cd	
Initial concentration	3000 mg/kg (5.34 meq 100 g^{-1})	
Initial soil pH	5.5	
Porosity	0.48	
Length of soil cell (cm)	15	
Applied current (mA)	100	
Electrical potential (V)	40	
Test duration (hr)	72	
Anode purging solution	Distilled water	0.001 M HNO$_3$
Cathode purging solution	Distilled water	0.1 M HNO$_3$

where z_i is the ionic charge of the species; F (C mol^{-1}) is the Faraday constant; R ($K^{-1}\ mol^{-1}$) is the ideal gas constant, and T (K) is the absolute temperature. By using the law of mass conservation, the transport of chemical species in porous media is described in Eq. 4 [13, 14, 17]:

$$n\frac{\partial c_i}{\partial t} = -\nabla . J_i + nG_i \quad ; \quad i = 1, 2, ..., N \tag{4}$$

$$G_i = G_i^{ad} + G_i^{aq} + G_i^p \tag{5}$$

where G_i (mol $m^{-3}\ s^{-1}$) describes the chemical reactions (as, e.g., precipitation, adsorption, or ionization). Where G_i^{aq} is the production rate of the ith aqueous chemical species due to aqueous phase reaction, G_i^{ad} is the production rate of the ith aqueous chemical species due to adsorption reaction, and G_i^p is the production rate of the ith aqueous chemical species because of precipitation reaction. In the mathematical model of ionic diffusion, we considered macroscopic Eqs. (1) to (4) where the influence of the physical phenomena at the microscopic and nanoscopic scales was included in the effective diffusion coefficient (Eq. 2) through the tortuosity factor [22]. The Poisson equation in electrostatics is used to complete the coupled system of equations,

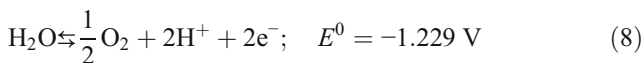$$\varepsilon \nabla^2 \varnothing + F \sum_i^N c_i z_i = 0 \tag{6}$$

where ε ($F\ m^{-1}$) is the permittivity of the medium. Under electroneutrality condition $\sum_{i=1}^{N} c_i z_i = 0$, and assuming the absence of magnetic forces, the electric field, E ($V\ m^{-1}$), is equal to the gradient of electrical potential $E = -\frac{\partial \varnothing}{\partial x}$. If we assume that in all of the simulation the electric field is constant, then Eq. 4 changes to Eq. 7 [10–13]:

$$n\frac{\partial c_i}{\partial t} = D_i^{\text{eff}} \frac{\partial^2 c_i}{\partial x^2} - \left(u_i^{\text{eff}} + k_{eo} \right) \frac{\partial c_i}{\partial x} E + nG_i \quad ; \quad i$$
$$= 1, 2, ..., N \tag{7}$$

2.3 Chemical Reactions

2.3.1 Electrolysis Reaction

We assumed that water electrolysis takes place at the electrode, water oxidation at the anode, and reduction at the cathode as:

$$H_2O \leftrightarrows \frac{1}{2}O_2 + 2H^+ + 2e^-; \quad E^0 = -1.229 \text{ V} \tag{8}$$

$$2H_2O + 2e^- \leftrightarrows H_2 + 2OH^-; \quad E^0 = -0.828 \text{ V} \tag{9}$$

where E^0 is the standard redox potential of the half reaction.

The electrolysis reactions produce the injection of protons and hydroxide ions from anode and cathode, respectively [3, 14].

2.4 Chemical Equilibrium

Having calculated transport equation numerically at each time step, the equilibrium concentration of each species was calculated from the last value obtained from the transport equation. Therefore, the water autoionization reaction between proton and hydroxide and precipitation reaction between cadmium and hydroxide were considered in the model. The chemical equilibrium of water is as follows:

$$H^+ + OH^- \leftrightarrows H_2O \quad K_w = [H^+][OH^-] = 10^{-14} \tag{10}$$

K_w (mol/L)^2 is the water equilibrium constant. The cadmium precipitation reaction is:

$$Cd^{2+} + 2OH^- \leftrightarrows Cd(OH)_2 \quad K_0 = [Cd^{2+}][OH^-]^2$$
$$= 5 \times 10^{-15} \tag{11}$$
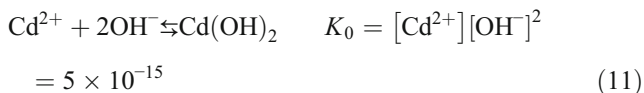
2.5 Adsorption Reaction

Adsorption is the net accumulation of chemical species at the interface between a solid phase and fluid (aqueous of gaseous) phase [23]. Adsorption of heavy metal ions and complexes on clay minerals occurs as a result of ion exchange, surface complexation, hydrophobic interaction, and electrostatic interaction [24]. Factors such as pH, nature and concentration of substrate and adsorbing ion, ionic strength, and the presence of complexing ions affect the extent of adsorption [25, 26].

Adsorption for ions, cadmium, and proton with a positive electrical charge was considered. For ions with negative electrical charge, OH^- and NO_3^-, adsorption was not considered due to kaolinite particles' negative surface charge. A linear function is the simplest and most widely used adsorption isotherm equation that was utilized to describe the adsorption of proton onto the kaolinite's surface in the present model. The adsorption isotherm equation is conventionally expressed in terms of the distribution coefficient:

$$G_i^{ad} = -\frac{\rho}{n}\frac{\partial c_i^{ad}}{\partial t} = -\frac{\rho}{n}\frac{\partial c_i^{ad}}{\partial c_i}\frac{\partial c_i}{\partial t} \tag{12}$$

$$\frac{\partial c_i^{ad}}{\partial c_i} = K_{di} \tag{13}$$

$$R_{di} = 1 + \frac{\rho K_{di}}{n} \tag{14}$$

where c_i^{ad} (mol kg^{-1}) is the amount of solute absorbed/adsorbed onto a unit weight of solid, c_i (mol m^{-3}) is the concentration of solute, K_{di} (m^3 kg^{-1}) is the distribution coefficient, ρ (kg m^3) is the bulk dry density of the soil, and R_{di} is the retardation factor. The equation that describes the transport of proton in the porous media of soil under EKR test with regard to retardation factor is:

$$n\frac{\partial c_{H^+}}{\partial t} = \frac{D_{H^+}^{eff}}{R_{dH^+}}\frac{\partial^2 c_{H^+}}{\partial x^2} - \left(\frac{u_{H^+}^{eff} + k_{eo}}{R_{dH^+}}\right)\frac{\partial c_{H^+}}{\partial x}E$$
$$+ \frac{n}{R_{dH^+}}G_{H^+}^{aq} \tag{15}$$

Yet, adsorption reactions for cadmium and proton are interactive when the pH value is the effective parameter in sorption species on soil. In the present model, an empirical data was used (Fig. 2) to model cadmium adsorption isotherm at different pH values and concentrations.

2.6 Numerical Analysis

The implicit finite difference scheme, Crank-Nicolson, was used to numerically solve the system of PDEs. The Crank-Nicolson is unconditionally stable [27]. Each transport equation for the target species should be solved numerically to find the concentration and pH profiles. Equation 7 is
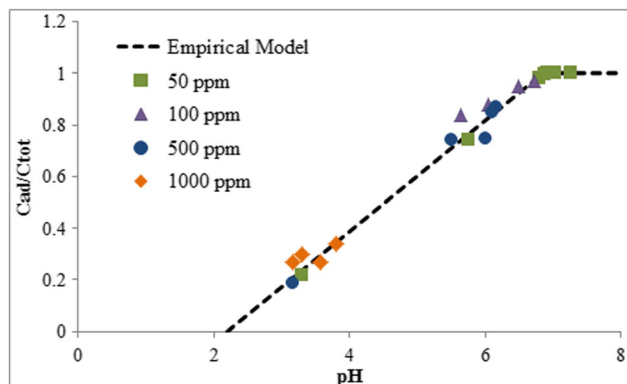

Fig. 2 Empirical cadmium adsorption isotherm model [10]

discretized to indicate how Crank-Nicolson was implemented in the transport equation:

$$\frac{c_k^{n+1} - c_k^n}{\Delta t} = 0.5\, A \left(\frac{c_{k-1}^n - 2c_k^n + c_{k+1}^n}{\Delta x^2} + \frac{c_{k+1}^{n+1} - 2c_k^{n+1} + c_{k+1}^{n+1}}{\Delta x^2} \right)$$
$$+ 0.5 B \left(\frac{c_{k+1}^n - c_{k-1}^n}{2\Delta x} + \frac{c_{k+1}^{n+1} - c_{k-1}^{n+1}}{2\Delta x} \right) \tag{16}$$

$$L = \begin{pmatrix} L_{1,1} & L_{1,2} & 0 & 0 & \cdots & 0 \\ -(S+0.5C) & 2(1+S) & -(S-0.5C) & \ddots & \ddots & \ddots \\ 0 & -(S+0.5C) & 2(1+S) & -(S-0.5C) & \ddots & \ddots \\ 0 & \ddots & \ddots & \ddots & \ddots & \ddots \\ \vdots & \ddots & \ddots & -(S+0.5C) & 2(1+S) & -(S-0.5C) \\ 0 & \ddots & \ddots & \ddots & L_{NX,NX-1} & L_{NX,NX} \end{pmatrix}_{NX \times NX} \tag{19}$$

$$T = \begin{pmatrix} T_{1,1} & T_{1,2} & 0 & 0 & \cdots & 0 \\ (S+0.5C) & 2(1-S) & (S-0.5C) & \ddots & \ddots & \ddots \\ 0 & (S+0.5C) & 2(1-S) & (S-0.5C) & \ddots & \ddots \\ 0 & \ddots & \ddots & \ddots & \ddots & \ddots \\ \vdots & \ddots & \ddots & (S+0.5C) & 2(1-S) & (S-0.5C) \\ 0 & \ddots & \ddots & \ddots & T_{NX,NX-1} & T_{NX,NX} \end{pmatrix}_{NX \times NX} \tag{20}$$

where $S = A\frac{\Delta t}{\Delta x^2}$ and $C = B\frac{\Delta t}{\Delta x}$. The elements, including $L_{1,1}$, $L_{1,2}$, $L_{NX, NX-1}$, $L_{NX, NX}$, $T_{1,1}$, $T_{1,2}$, $T_{NX, NX-1}$, and $T_{NX, NX}$, were generated from the boundary conditions. In the EKR process, the use of the Neumann boundary (insulated boundary) and the Dirichlet boundary cannot describe the nature of the EKR which is due to the existence of flux at the boundaries caused by electrode reaction and advection of fluid [3]. Boundary conditions for the PDEs were completed by considering species flux and electrolysis reaction at the electrodes [28]:

$$-D_i^{\mathrm{eff}} \frac{\partial c_i}{\partial x} + \left(k_{eo} + u_i^{\mathrm{eff}}\right)\left(-\frac{\partial \varnothing}{\partial x}\right) c_i \Big|_{x=0}$$
$$= c_i^p k_{eo}\left(-\frac{\partial \varnothing}{\partial x}\right) + \frac{I}{z_i F} \tag{21}$$

$$-D_i^{\mathrm{eff}} \frac{\partial c_i}{\partial x} + \left(k_{eo} + u_i^{\mathrm{eff}}\right)\left(-\frac{\partial \varnothing}{\partial x}\right) c_i \Big|_{x=L}$$
$$= c_i^p k_{eo}\left(-\frac{\partial \varnothing}{\partial x}\right) + \frac{I}{z_i F} \tag{22}$$

where $A = D_i^{\mathrm{eff}}/n$; $B = \frac{\left(u_i^{\mathrm{eff}} + k_{eo}\right)}{n}(-E)$; Δx and Δt are the spatial and the time increments, respectively. The final form of Eq. 16 is:

$$-(S+0.5C)c_{k-1}^{n+1} + 2(1+S)c_k^{n+1} - (S-0.5C)c_{k+1}^{n+1}$$
$$= (S+0.5C)c_{k-1}^n + 2(1-S)c_k^n + (S-0.5C)c_{k+1}^n \tag{17}$$

$$Lc^{n+1} = Tc^n \tag{18}$$

where I (A m^{-2}) is the electric current density and c_i^p is the concentration of specific ions in purging solution. The whole electric current is expended in generation of H$^+$ at the anode and OH$^-$ at the cathode, and for cadmium, no electrolysis reaction was considered.

By imposing electroneutrality into the system of equations, it is possible to achieve NO$_3^-$ concentration at each time and space by:

$$C_{NO} = -\frac{\sum_{j=1}^{3} z_j c_j}{z_{NO}} \tag{23}$$

In our numerical simulation, we implemented 1 mm for spatial and 10 s for time increment. The electroosmotic permeability (k_{eo}) in soils is in the range of 10^{-5} to 10^{-4} cm^2 s^{-1} V^{-1} [19]. k_{eo} was set equal to 4×10^{-9} (m^2 V^{-1} s^{-1}), and similar to other researchers, it was kept constant during the simulation [8, 10–12, 14]. The tortuosity factor (τ) for kaolinite varies over a range of 0.12–0.5 [18], and it was set equal to 0.3. The sensitivity analysis of retardation factor was carried out to find the best fit with the experimental measurement. Table 2 indicates the input parameters in the present model.

Table 2 Input parameters in the model

Parameter	Value	Reference
D_{H^+} (m²/s)	93.1×10^{-10}	[29]
D_{OH^-} (m²/s)	52.7×10^{-10}	[29]
$D_{Cd^{2+}}$ (m²/s)	7.19×10^{-10}	[29]
$D_{NO_3^-}$ (m²/s)	19.0×10^{-10}	[29]
$u_{H^+}^{eff}$ (m²/V s)	5.22×10^{-8}	Eq. 3
$u_{OH^-}^{eff}$ (m²/V s)	2.96×10^{-8}	Eq. 3
$u_{Cd^{2+}}^{eff}$ (m²/V s)	1.06×10^{-8}	Eq. 3
$u_{NO_3^-}^{eff}$ (m²/V s)	1.071×10^{-10}	Eq. 3
Retardation factor (R_d)	5	–
Tortuosity factor (τ)	0.3	–
Electroosmotic permeability (k_{eo}) (m² V⁻¹ s⁻¹)	4×10^{-9}	–

2.7 Model Efficiency

The coefficient of determination (R^2) and index of agreement (IA) indicate the efficiency of simulation predictions [30]. To indicate the accuracy and efficiency of the models, R^2 and IA were calculated between our numerical simulation results and the experimental measurement. We also computed the R^2 and IA between Kim et al. [10] simulation results and their experimental measurement. The R^2 and IA vary between zero and one. When the R^2 and IA approach to one, the model is well developed. The R^2 and IA formulations are:

$$R^2 = \left(\frac{\sum_{i=1}^{n} \left(O_i - \overline{O} \right) \left(P_i - \overline{P} \right)}{\sqrt{\sum_{i=1}^{n} \left(O_i - \overline{O} \right)^2} \sqrt{\sum_{i=1}^{n} \left(P_i - \overline{P} \right)^2}} \right)^2 \tag{24}$$

$$IA = 1 - \frac{\sum_{i=1}^{n} (O_i - P_i)^2}{\sum_{i=1}^{n} \left(\left| P_i - \overline{O} \right| + \left| O_i - \overline{O} \right| \right)^2} \tag{25}$$

where O is the observed value (experimental measurement), $\overline{O}$ is the mean value of O, P is the predicted value (numerical simulation result), and $\overline{P}$ is the mean value of P.

3 Results and Discussion

Figures 3 and 4 illustrate the comparison between our model prediction, the experimental data and Kim et al.'s [10] numerical simulation for pH along the soil medium for unenhanced and acid-enhanced tests, respectively. Due to the electrolysis reaction, protons and hydroxide ions enter into the soil and change the pH of the soil. In the unenhanced test, the pH of the soil near the anode compartment decreased to pH < 2, and near the cathode compartment increased to pH > 11 [7, 9–11, 14, 31]. A pH jump is observable in Fig. 3, and this jump happens when acid and base front meet each other. The jump is close to the cathode compartment, because the ionic mobility of proton is greater than hydroxide ion; in addition, the electroosmotic flow direction is from the anode to the cathode compartment. Consequently, the transport velocity of the acid front is greater than the base front. In the acid-enhanced test, the hydroxide ions are neutralized by dropping acid into the cathode compartment. This happens because of the chemical reaction between the hydroxide ions and nitric acid; thus, OH⁻ ions do not enter into the soil medium to increase.

For the purpose of comparison, retardation factor was set equal to 4.6, which is the value that Kim et al. [10] selected in their simulation. Based on the sensitivity analysis, when retardation factor was equal to 5, the best fit to the experimental
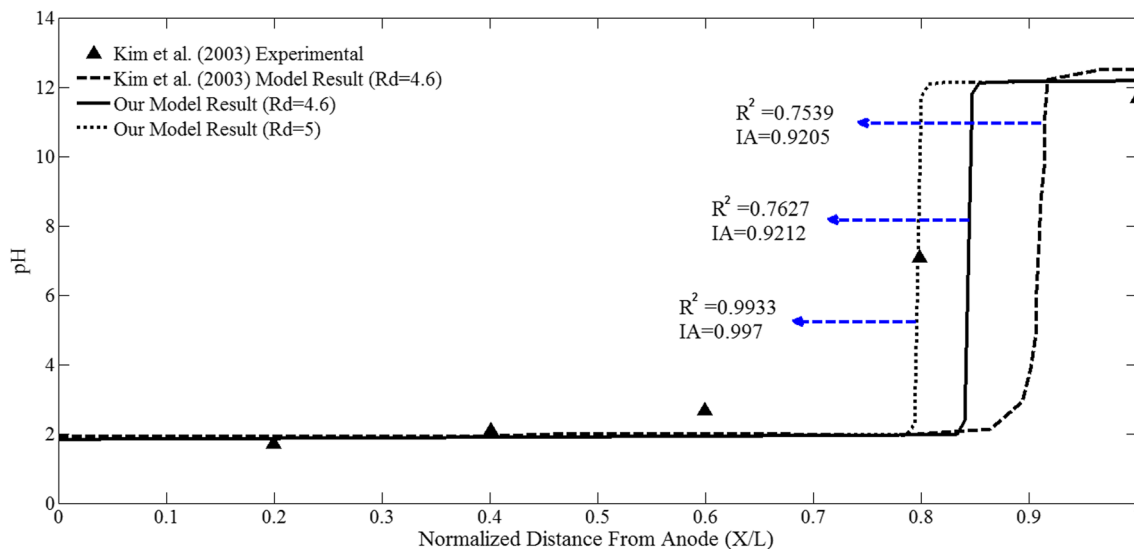

Fig. 3 The predicted and the measured pH profile along the soil sample after 3 days of unenhanced EKR
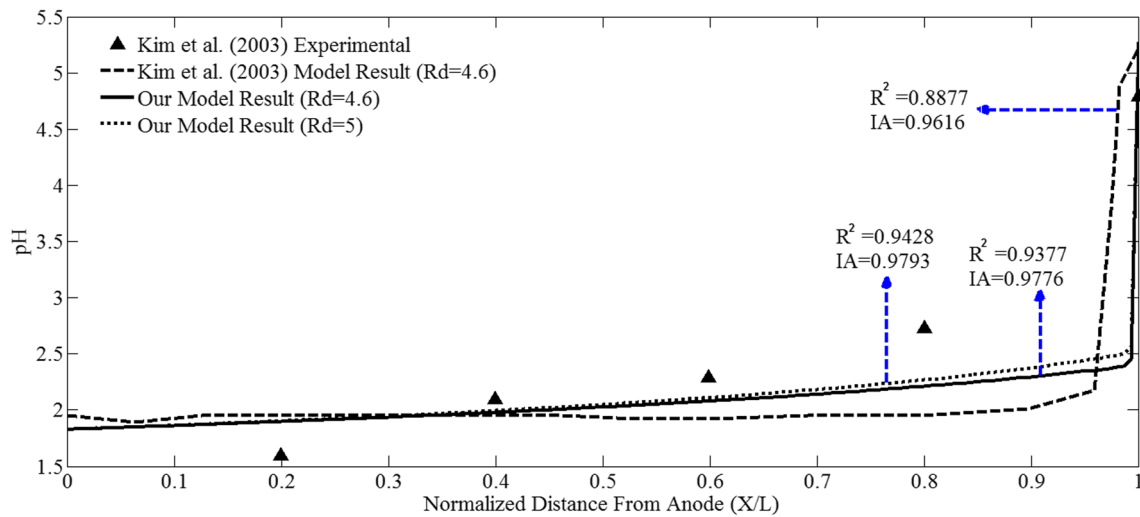
Fig. 4 The predicted and the measured pH profile along the soil sample after 3 days of acid-enhanced EKR

measurement was achieved. By setting a retardation factor equal to 4.6, the value that Kim et al. [10] used in their model, according to R^2 and IA calculation, our model showed better prediction than Kim et al.'s [10] model.

This difference could be resulted from the use of different numerical schemes and different boundary conditions. The main transport mechanisms in the electrokinetic soil remediation process are electroosmotic flow, ionic migration, and diffusion, which were taken into consideration in the present model. These transport mechanisms lead to a set of partial differential equations that describe the transport process. In all of the models which have been presented up to now, these transport phenomena have been considered to simulate the process. Therefore, the governing equation cannot be different.

In addition to numerical method which is different, the difference between the present work and Kim et al.'s model is the use of different boundary conditions. Kim et al. [10] used algebraic boundary conditions for proton and hydroxide ions in their model, which were based on their experimental observation. However, we used the boundary conditions in our model which were generated based on the equality between the flux of solute on the inside and immediately outside of the soil column. These boundary conditions are developed according to the mathematical formulation, not an experimental observation.

According to R^2 and IA calculation, the best match to the experiment is achieved by setting retardation factor equal to 5. Kim et al. [10] on the basis of Alshawabkeh and Acar's [8] recommendation selected retardation factor equal to 4.6. Alshawabkeh and Acar [8] calculated this value according to acid front transport rate. They computed theoretical acid front transport rate as equal to 4.6 cm/day and observed it 1 cm/day.
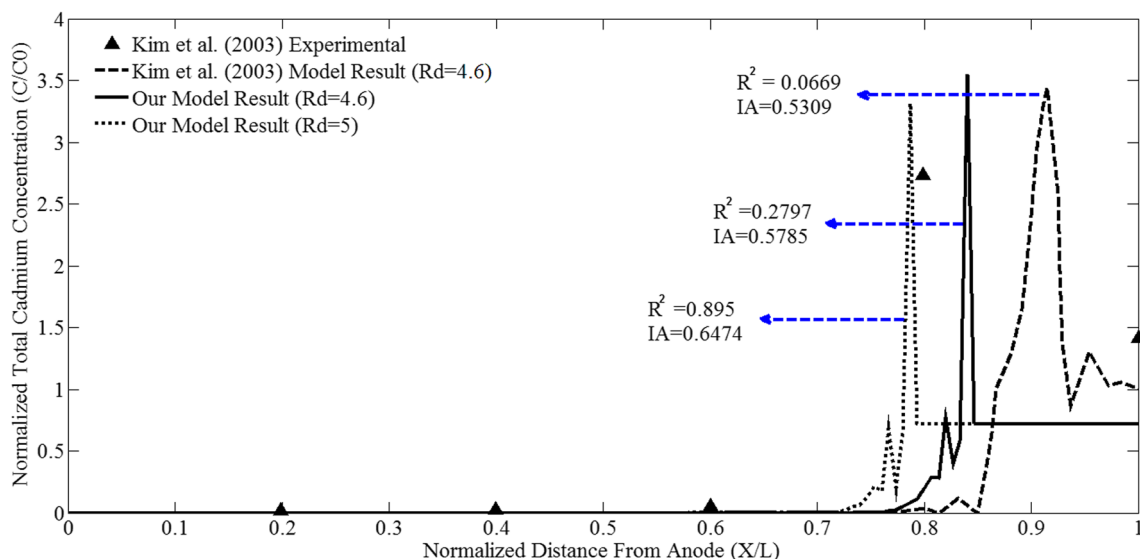

Fig. 5 The predicted and the measured cadmium concentration along the soil sample after 3 days of unenhanced EKR
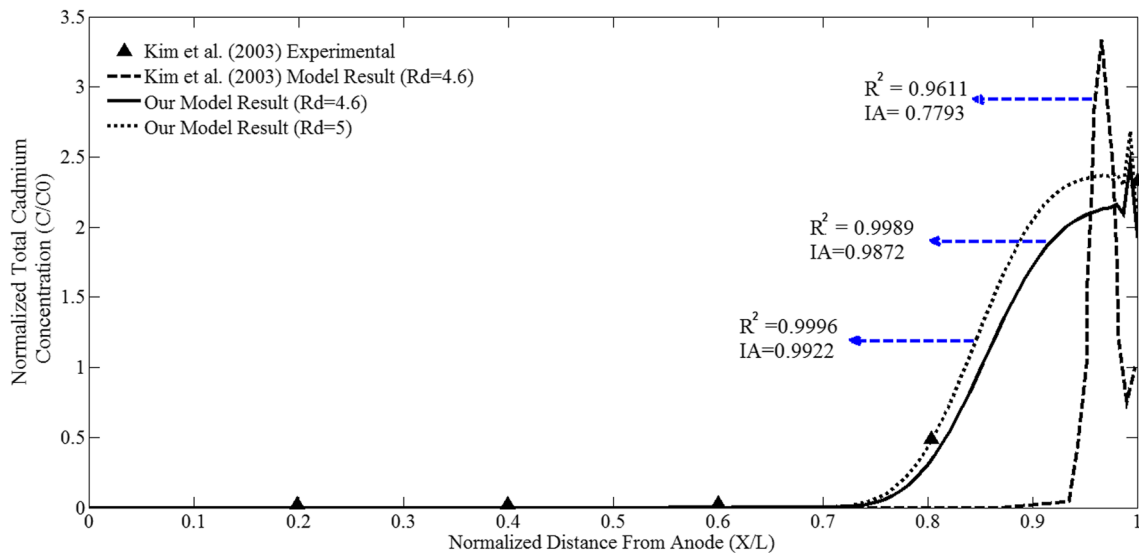
Fig. 6. The predicted and the measured cadmium concentration along the soil sample after 3 days of acid-enhanced EKR

They divided the theoretical value by experimental value and introduced retardation factor equal to 4.6. Alshawabkeh and Acar [8] calculated theoretical acid front transport rate based on effective ionic mobility. Effective ionic mobility is a function of porosity, tortuosity, and ionic mobility ($u_i^{\mathrm{eff}} = n\tau u_i$). Suitable estimation of porosity and tortuosity is important, yet the critical factor is the use of ionic mobility at infinite dilution [16]. It is established in electrochemistry that ionic mobility is dependent on the ionic strength of the solution. Therefore, the use of ionic mobility at infinite dilution for measuring the effective ionic mobility needs further investigation [16]; then, it can be concluded that the value equal to 4.6 is not an exact number.

Figures 5 and 6 illustrate the present model's result, as well as numerical prediction and experimental data of Kim

et al. [10], for cadmium concentration profile in unenhanced and acid-enhanced tests, respectively. In the figures, C defines cadmium concentration in the soil after remediation ,and C_0 is cadmium concentration before remediation. According to linear and pH-dependent adsorption isotherm (Fig. 2), at the beginning of the tests, 72% of cadmium ions in the soil was adsorbed and 28% was in aqueous form. By running the program and transferring proton ions into the soil medium, the pH decreased, and cadmium ions desorbed from the kaolinite surface could transport across the soil porous media. In the unenhanced test, cadmium ions transported and accumulate in the alkaline zone where pH had a jump and acid and base front met each other. In the acid-enhanced test due to the reaction between hydroxide and nitric acid, counterion entered into
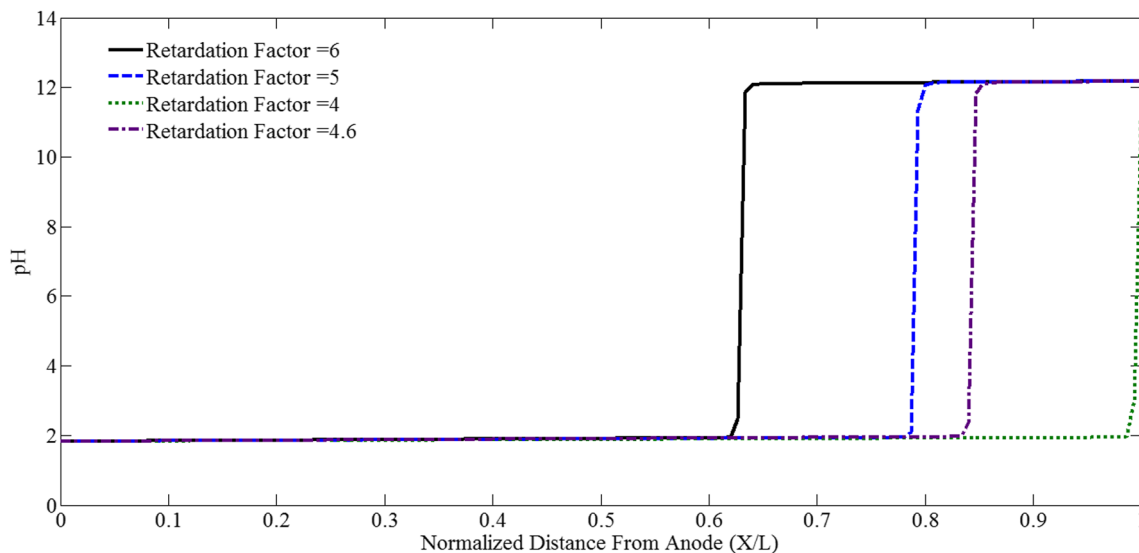

Fig. 7 The effect of changing retardation factor in the pH prediction after 3 days of unenhanced EKR
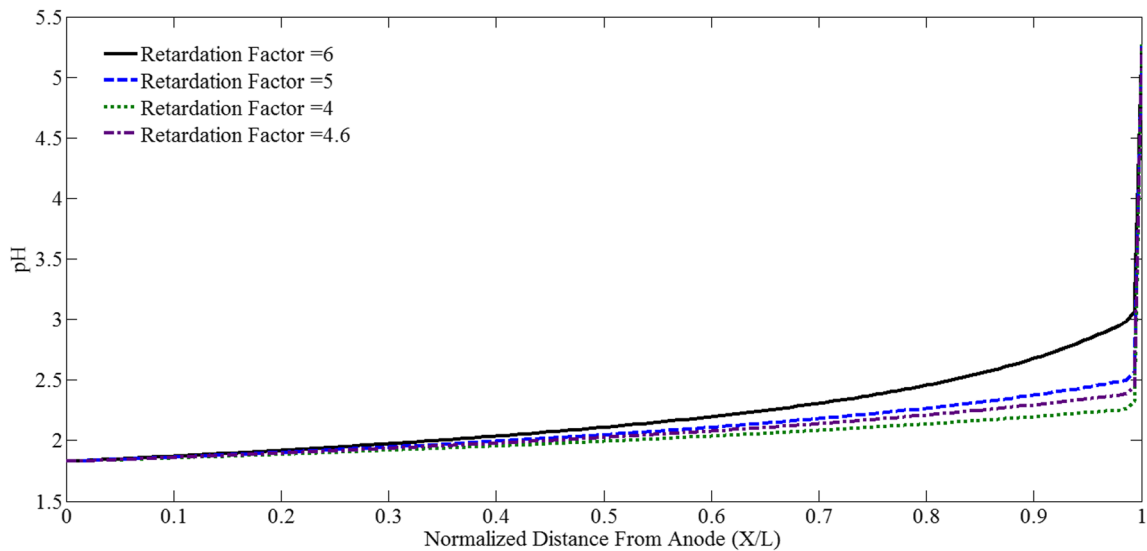
Fig. 8 The effect of changing retardation factor in pH prediction after 3 days of acid-enhanced EKR

the soil rather than hydroxide. Therefore, pH near the cathode compartment is lower than initial soil pH, and the cadmium ions in the acidic condition could transport in the soil more freely in comparison with the unenhanced test. Furthermore, the cadmium accumulated in the soil close to the cathode compartment. The straight solid curve in Fig. 5 is due to pH condition in this zone. Under the extreme basic condition, cadmium ions are adsorbed or precipitated without transportation in the soil medium. In the acidic condition, cadmium ions could transport in the soil freely. As explained before, when acid and base front meet each other, a jump happens in the cadmium concentration profile, and cadmium ions transported in the soil are accumulated in this zone, and this phenomenon is consistent with other researchers' studies [11, 13]. Moreover, as observable in Fig. 5, jumps in the cadmium concentration for

each curve is consistent with the zone when acid and base front meet each other (transient pH profile) in Fig. 3.

Similar to pH prediction, we set retardation factor equal to 4.6 to compare our model prediction with the Kim et al.'s [10] model and then selected the retardation factor equal to 5. As indicated in Figs. 5 and 6, the present implicit finite difference model has a better simulation result related to Kim et al.'s [10] model. Moreover, according to R^2 and IA calculation, the best fit with the experimental measurement was achieved by the present implicit finite difference model with setting retardation factor equal to 5.

3.1 Sensitivity Analysis

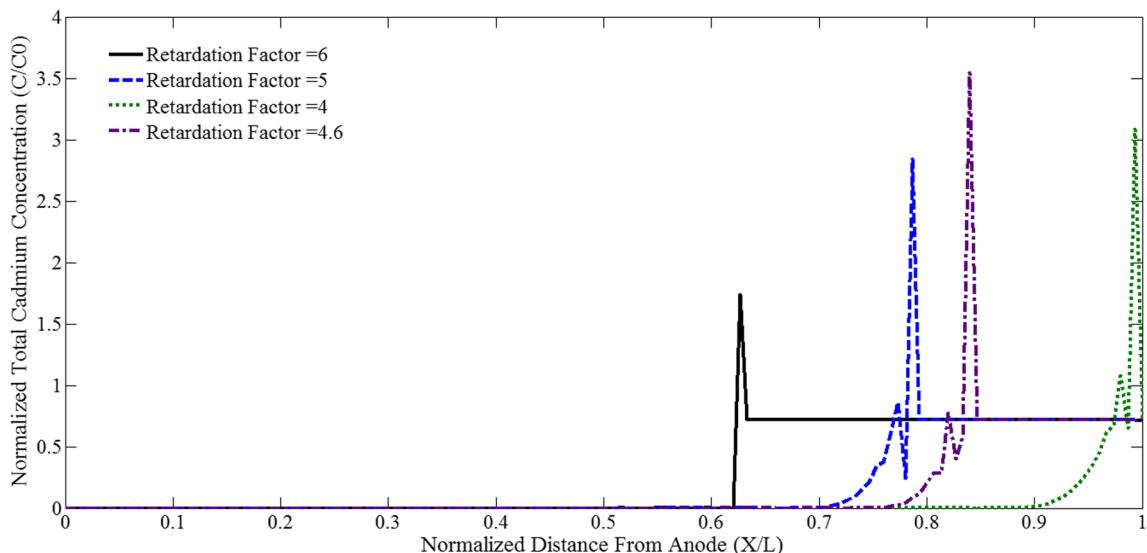The sensitivity analysis was carried out by changing retardation and tortuosity factors to identify the role of these

Fig. 9 The effect of changing retardation factor on the cadmium concentrations profile after 3 days unenhanced EKR
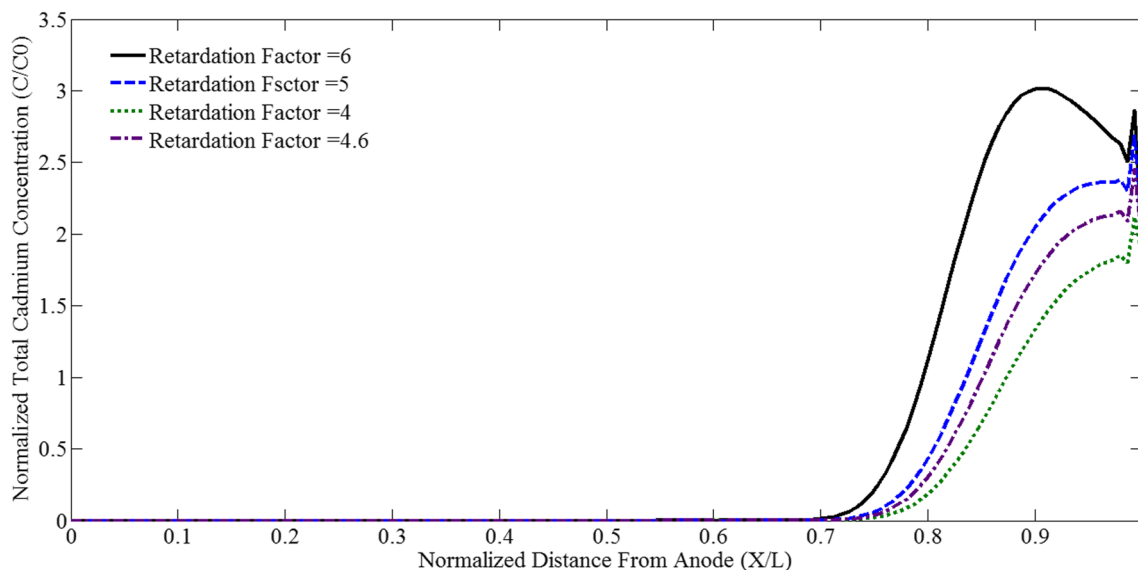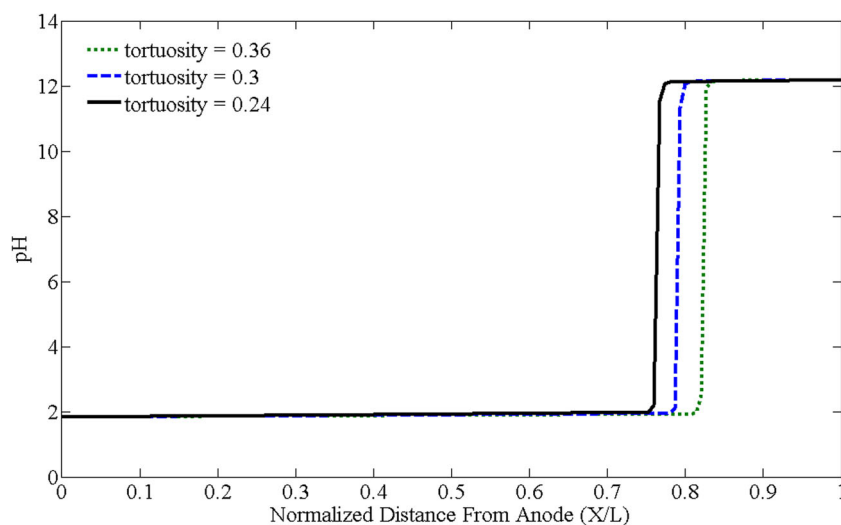
Fig. 10 The effect of changing retardation factor on the cadmium concentrations profile after 3 days of acid-enhanced EKR

parameters on the model outputs. We either increased or decreased retardation and the tortuosity factor by 20% to identify the role of these parameters in the removal of cadmium and pH profile, while other input parameters kept constant. At the first stage, the retardation factor was changed to understand its effect on the model output. Figures 7 and 8 represent the effect of changing retardation factor on the pH prediction in unenhanced and acid-enhanced tests, respectively. In the unenhanced test, increasing retardation factor ($R_d = 6$) reduced the transport velocity of the acid front; therefore, the base front could progress in the soil more than when selecting $R_d = 5$. Decreasing retardation factor ($R_d = 4$) increased the velocity of the acid front and whole of the soil got acidified. In the acid-enhanced test, increasing and decreasing retardation factor had a direct impact on the acid front movement velocity, yet because of neutralization of hydroxide ions in the cathode chamber, the hydroxide did not enter into the soil medium.

Consequently, pH profile was not affected drastically by changing retardation factor.

Figures 9 and 10 demonstrate the impact of changing retardation factor on the cadmium concentration profile. In the unenhanced test, when retardation factor was equal to 4, the whole of the soil was acidified, the rate of adsorption and precipitation reactions decreased, and cadmium transportation in the soil accelerated. Consequently, cadmium accumulated close to the cathode compartment. By increasing retardation factor, the acid front movement reduced, and in the alkaline condition, cadmium adsorption and precipitation were increased. Also, the similar procedure can be observed for the acid-enhanced test (Fig. 10). The cadmium concentration profile did not change considerably because of small changes in the pH profile.

Figures 11 and 12 depict the effect of changing tortuosity on the pH prediction profile for unenhanced and acid-

Fig. 11 The effect of changing tortuosity on the pH prediction profile after 3 days of unenhanced EKR

Fig. 12 The effect of changing tortuosity on the pH prediction after 3 days of acid-enhanced EKR
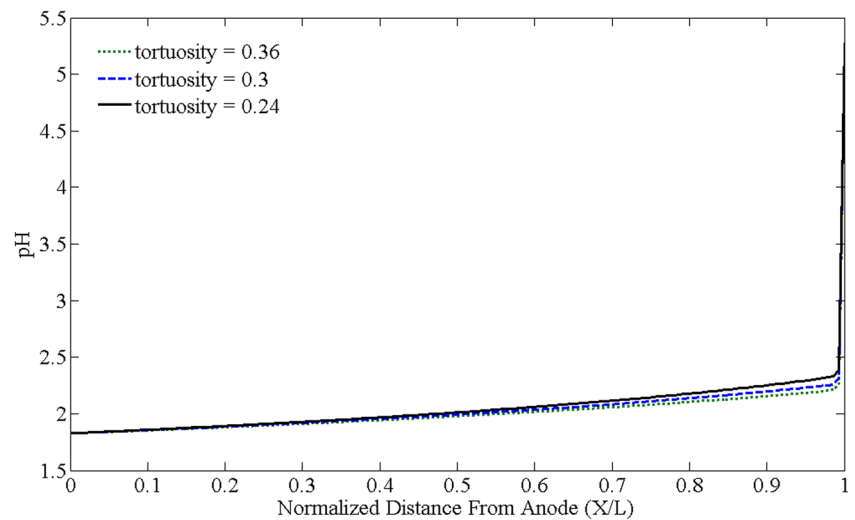
enhanced tests, respectively. In the unenhanced test, by increasing tortuosity 20% ($\tau = 0.36$), the acid front moved a bit faster, and the pH jump occurred a bit closer to the cathode. In contrast, by decreasing tortuosity 20% ($\tau = 0.24$), the acid front moved a bit slower, and the pH jump occurred a bit farther to the cathode. Likewise, in the enhanced test, increasing tortuosity factor accelerated the acid front movement (pH in the soil got a bit more acidified) and decreasing tortuosity factor decreased acid front movement (pH in the soil tended to initial soil pH).

Figures 13 and 14 demonstrate the effect of tortuosity factor on the cadmium concentration profile in the unenhanced and acid-enhanced tests, respectively. By increasing the tortuosity factor, the cadmium effective ionic mobility and then its velocity increased and by decreasing the tortuosity factor the cadmium effective ionic mobility and then its velocity decreased. Therefore, increasing tortuosity led to more cadmium removal prediction and decreasing tortuosity led to the less

cadmium removal prediction by the model in the unenhanced and acid-enhanced tests.

Tables 3 and 4 present the result of the sensitivity analysis on the pH and cadmium concentration profiles, respectively. According to Tables 3 and 4, changing retardation factor had a more significant impact on the unenhanced test than the acid-enhanced test. In the acid-enhanced test, dropping acid into the cathode chamber neutralized the OH^- ions, and pH near cathode did not change. In unenhanced test, since retardation factor has a direct impact on the proton movement in the soil sample, increasing and decreasing retardation factor led to considerable pH changes, because the increasing retardation factor resulted in less acid front movement and more base front progress. On the other hand, decreasing retardation factor resulted in more acid front movement and less base front progress.

The result of sensitivity analysis indicated that changing tortuosity factor has a more noticeable impact on the cadmium

Fig. 13 The effect of changing tortuosity factor in the cadmium concentration profile after 3 days unenhanced EKR
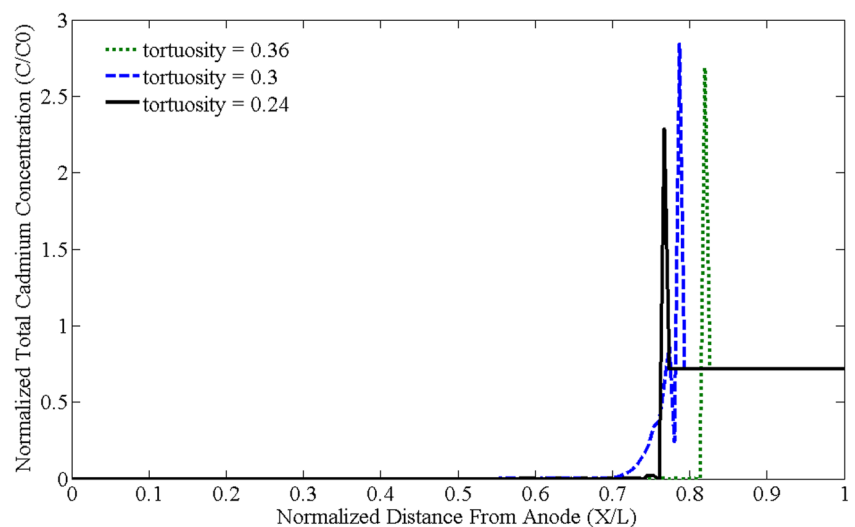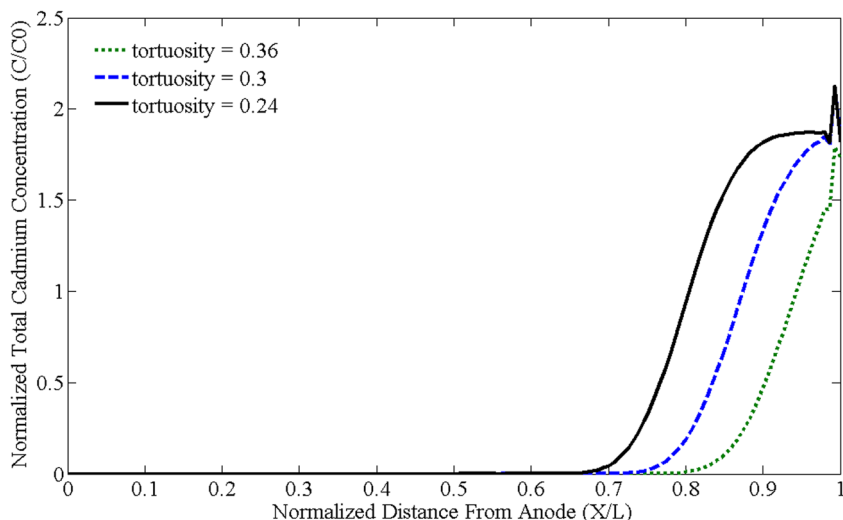
Fig. 14 The effect of a changing tortuosity factor in the cadmium concentration profile after 3 days of acid-enhanced EKR

concentration profile than pH profile. Changing tortuosity has a direct impact on the ionic mobility of cadmium which is the main transport mechanism of cadmium. Conversely, pH was not affected by tortuosity very much, and this could be due to the same impact that tortuosity had on proton and hydroxide ionic mobility.

4 Conclusions

In the present study, a mathematical model based on an implicit finite difference method was introduced to describe the electrokinetic remediation of cadmium-contaminated soil. We used a set of partial differential equations and algebraic equations to simulate the EKR process. Different geochemical reactions including precipitation/dissolution, adsorption/desorption, and water auto ionization reaction were applied. In addition, realistic boundary conditions considering the effect of electrolysis and flux on the boundaries were implemented in the model. The simulation results were compared with the existing experimental data, as well as available explicit finite difference model. The key conclusion summarized as follows:

Table 4 The sensitivity analysis of tortuosity and retardation factors (cadmium concentration profile)

Parameters		R^2			IA		
		Changing data		Best fit	Changing data		Best fit
		+ 20%	− 20%		+ 20%	− 20%	
Unenhanced	Retardation factor	0.837	0.0669	0.895	0.646	0.5113	0.6474
	Tortuosity	0.85	0.0669	0.895	0.647	0.5113	0.6474
Acid-enhanced	Retardation factor	0.896	0.99	0.9996	0.97	0.9763	0.9922
	Tortuosity	0.904	0.9611	0.9996	0.9668	0.9552	0.9922

Table 3 The sensitivity analysis of tortuosity and retardation factors (pH profile)

Parameters		R^2			IA		
		Changing data		Best fit	Changing data		Best fit
		+ 20%	− 20%		+ 20%	− 20%	
Unenhanced	Retardation factor	0.85	0.7522	0.9933	0.9297	0.9161	0.997
	Tortuosity	0.854	0.7538	0.9933	0.931	0.9176	0.997
Acid-enhanced	Retardation factor	0.8877	0.9263	0.9428	0.9616	0.9733	0.9793
	Tortuosity	0.9355	0.923	0.9428	0.975	0.971	0.9793

1- In the unenhanced test, while retardation factor was 5, the calculated R^2 and IA between our model prediction for cadmium concentration profile and the experimental data were 0.895 and 0.6474, respectively. In the acid-enhanced test, R^2 and IA calculation between our model result and the experiment were 0.9996 and 0.9922, respectively. This indicates that a good agreement between our model and the experimental data.

2- In the unenhanced test, while retardation factor was 5, the calculated R^2 and IA between our model output for pH profile and the experimental data were 0.9933 and 0.997, respectively. In the acid-enhanced test, R^2 and IA calculation between our model result and the experiment were 0.9428 and 0.9723, respectively, which indicates a good agreement between our model and the experimental data.

3- The results of our implicit finite difference model, through setting retardation factor equal to 4.6, were more precise in comparison with Kim et al.'s [10] explicit models for cadmium concentration profile.

4- The results of our model, through setting retardation factor equal to 4.6, were more accurate in comparison with Kim et al.'s [10] model for pH profile.

5- Comparing with Kim et al.'s model, we used different numerical scheme and boundary conditions in the proposed model which could be responsible for better prediction result. In the present model, boundary conditions used developed based on the mathematical simulation rather than an experimental observation.

6- The sensitivity analysis of retardation factor indicated that changing retardation factor had a more significant impact on the unenhanced test than the acid-enhanced test.

7- The sensitivity analysis of tortuosity factor indicated that changing tortuosity factor had a negligible effect on the pH profile, though it has a non-negligible effect on the cadmium concentration profile.

References

1. Mascia, M., Palmas, S., Polcaro, A. M., Vacca, A., & Muntoni, A. (2007). Experimental study and mathematical model on remediation of Cd spiked kaolinite by electrokinetics. *Electrochimica Acta, 52*, 3360–3365.

2. H. D. Sharma and K. R. Reddy, Geoenvironmental engineering: site remediation, waste containment, and emerging waste management technologies, *Wily*, 2004. [Online]. Available: http://eu.wiley.com/WileyCDA/WileyTitle/productCd-0471215996.html. [Accessed: 29-Jan-2015].

3. K. R. Reddy and C. Cameselle, Electrochemical remediation technologies for polluted soils, sediments and groundwater.

4. Reddy, K. R., & Chinthamreddy, S. (2003). Sequentially enhanced electrokinetic remediation of heavy metals in low buffering clayey soils. *J. Geotech. Geoenvironmental Eng., 129*(3), 263–277.

5. Vereda-Alonso, C., Rodríguez-Maroto, J. M., García-Delgado, R. A., Gómez-Lahoz, C., & García-Herruzo, F. (2004). Two-dimensional model for soil electrokinetic remediation of heavy metals: application to a copper spiked kaolin. *Chemosphere, 54*, 895–903.

6. Acar, Y. B., & Alshawabkeh, A. N. (1993). Principles of electrokinetic remediation. *Separation Science and Technology, 27*(13), 2638–2674.

7. Jacobs, R. A., Sengun, M. Z., Hicks, R. E., and Prostien, R. F. (1994) Model and Experiments on soil remediation by electric fields, no. November 2012, pp. 129–147.

8. Alshawabkeh, A. N. and Acar, Y. B. (1996) Electrokinetic remediation. II: theoretical model, *Journal of Geotechnical Engineering*, pp. 186–196.

9. Haran, B. S., Popov, B. N., Zheng, G., & WWhite, R. E. (1997). Mathematical modeling of hexavalent chromium decontamination from low surface charged soils. *Journal of Hazardous Materials, 55*(97).

10. Kim, S. O., Kim, J. J., Yun, S. T., and Kim, K. W. (2003) Numerical and experimental studies on cadmium(II) transport in kaolinite clay under electrical fields, *Water, Air Soil Pollut.*, vol. 150, no. Ii, pp. 135–162.

11. Kim, S., Kim, J., Kim, K., & Yun, S. (2004). Models and experiments on electrokinetic removal of Pb(II) from kaolinite clay. *Separation Science and Technology, 39*(8), 1927–1951.

12. Park, J. S., Kim, S. O., Kim, K. W., Kim, B. R., & Moon, S. H. (2003). Numerical analysis for electrokinetic soil processing enhanced by chemical conditioning of the electrode reservoirs. *Journal of Hazardous Materials, 99*, 71–88.

13. Al-Hamdan, A. Z., & Reddy, K. R. (2008). Electrokinetic remediation modeling incorporating geochemical effects. *Journal of Geotechnical and Geoenvironmental Engineering, 134*, 91–105.

14. Paz-García, J. M., Johannesson, B., Ottosen, L. M., Ribeiro, A. B., & Rodríguez-Maroto, J. M. (2011). Modeling of electrokinetic processes by finite element integration of the Nernst-Planck-Poisson system of equations. *Separation and Purification Technology, 79*, 183–192.

15. Yeung, A. T., non Hsu, C., & Menon, R. M. (2011). Electrokinetic extraction of lead from kaolinites: I. Numerical modeling. *Environmentalist, 31*, 26–32.

16. Paz-Garcia, J. M., Baek, K., Alshawabkeh, I. D., & Alshawabkeh, A. N. (2012). A generalized model for transport of contaminants in soil by electric fields. *Journal of Environmental Science and Health. A. Tox. Hazard Subst Environmental Engineering, 47*, 308–318.

17. Asadollahfardi, G., Rezaee, M., and Tavakoli Mehrjardi, G. (2016). Simulation of unenhanced electrokinetic process for lead removal from kaolinite clay, *International Journal of Civil Engineering*.

18. Alshawabkeh, A. N. (1994). *Theoretical and experimental modeling of removing contaminants from soils by an electric field*. The Louisiana State University.

19. Mitchell, J. K. (1993). Fundamentals of soil behavior. Wiley.

20. Probstein, R. F. (1994). Physicochemical hydrodynamics—an introduction.

21. Holmes, P. (1962). Electrochemistry of semiconductors.

22. Bourbatache, K., Millet, O., & Aït-Mokhtar, A. (2012). Ionic transfer in charged porous media. Periodic homogenization and parametric study on 2D microstructures. *International Journal of Heat and Mass Transfer, 55*(21–22), 5979–5991.

23. Sposito, G. (1989). *The chemistry of soils*. Second: Oxford University Press.

24. Hizal, J., & Apak, R. (2006). Modeling of cadmium(II) adsorption on kaolinite-based clays in the absence and presence of humic acid. *Applied Clay Science, 32*, 232–244.

25. Ikhsan, J., Johnson, B., & Wells, J. (1999). A comparative study of the adsorption of transition metals on kaolinite. *Journal Colloid and Interface Science, 217*(2), 403–410.

26. P. Srivastava, B. Singh, and M. Angove, Competitive adsorption behavior of heavy metals on kaolinite, Journal of Colloid and Interface Science, vol. 290, no. 2005, pp. 28–38, 2005.

27. Fletcher, C. A. J. (1998). Computational techniques for fluid dynamics 1—fundamental and general techniques.

28. Shapiro, A. P. (1990). Electroosmotic purging of contaminants from saturated soils, Massachusetts Institute of Technology.

29. Lide, D. R. (2009). CRC Handbook of Chemistry and Physics.

30. Asadollahfardi, G., Darban, A. K., Noorifar, N., & Rezaee, M. (2016). Mathematical simulation of surfactant flushing process to remediate diesel contaminated sand column. *Advances in Environmental Research, 5*(4), 213–224.

31. Asadollahfardi, G., Nasrollahi, M., Rezaee, M., & Khodadadi Darban, A. (2017). Nickel removal from low permeable kaolin soil under unenhanced and EDTA-enhanced electrokinetic process. *Advances in Environmental Research, 2*, 147–158.